Journal of Scientific & Industrial Research
Vol. 84, November 2025, pp. 1241-1253
DOI: 10.56042/jsir.v84i11.21774

Turbulence Modelling and Flow Analysis of a Trapped Vortex Combustor

Dinesh Keloth Kaithari[1], Gulab Dattrao Siraskar[2], Ramdas Biradar[3], Sachin Kandharkar[4]*, Ganesh E. Kondhalkar[5], Prabhakar N. Kota[6], Anant Sidhappa Kurhade[7,8]* & Shital Yashwant Waware[7,8]

[1]Department of Mechanical and Industrial Engineering, College of Engineering, National University of Science and Technology, Muscat, Oman

[2]Department of Mechanical Engineering, PCET's Pimpri Chinchwad College of Engineering and Research, Ravet, Pune 412 101, Maharashtra, India

[3]School of Engineering and Technology, PCET's Pimpri Chinchwad University, Pune 412 106, Maharashtra, India

[4]Department of Mechanical Engineering, Modern Education Society's Wadia College of Engineering, Pune 411 001, Maharashtra, India, Affiliated to Savitribai Phule Pune University, Pune

[5]Department of Mechanical Engineering, ABMSP's Anantrao Pawar College of Engineering and Research, Parvati, Pune 411 009, Maharashtra, India

[6]Department of Electronics and Telecommunication Engineering, Modern Education Society's Wadia College of Engineering, Pune 411 001, Maharashtra, India, Affiliated to Savitribai Phule Pune University, Pune

[7]Department of Mechanical Engineering, Dr. D. Y. Patil Institute of Technology, Sant Tukaram Nagar, Pimpri, Pune 411 018, Maharashtra, India

[8]Dnyaan Prasad Global University (DPGU), School of Technology and Research Dr. D. Y. Patil Unitech Society, Sant Tukaram Nagar, Pimpri, Pune, 411 018, Maharashtra, India

Received 18 July 2025; revised 26 November 2025; accepted 09 December 2025

In this paper, a computational study is presented on the turbulence structure and aerodynamics of a Trapped Vortex Combustor (TVC) by means of Reynolds–Averaged Navier–Stokes (RANS) calculations. The aim is to assess the ability of three turbulence models — RSM, Realizable k—ε and SST—kω — in predicting flow characteristics and pressure drop within the combustor. Fluent of ANSYS was used to simulate the scratching process under different Reynolds numbers and cavity geometries, and simulation results were compared with data from literature. A grid insensitivity analysis demonstrated 30,000 cells to be the optimum mesh refinement. It is also found from the results that RSM model provides the best predictions of pressure loss and gives a maximum discrepancy slightly above 12.1% compared SST—kω (23.9%) and Realizable k—ε (26.7%). Parametric studies showed that for Reynolds numbers up to 300% the recirculation zone would strengthen factor of three and turbulence intensity by an order of magnitude, respectively, while flow imprints did not show a considerable shift. The authors suggest an optimum H/Df ratio of the depth—to—flow diameter is found to be around 0.6, where a pressure drop reduction (to less than one—third) due to vortex generation inside and downstream of the cavity is minimum. Both small (H/Df 1) cavities generate multiple vortices, resulting in higher aerodynamic losses. The novelty is to compare RANS models for TVC optimization and determine Reynolds number and cavity geometry effects. These results provide useful information for the design and optimization of TVC—based propulsion systems, highlighting the significance of turbulence model and combustor geometry in favoring combustion efficiency and stability.

Keywords: ANSYS fluent, Cavity geometry effects, Numerical computations, RANS models, Trapped vortex combustion

Introductions

Trapped Vortex Combustion (TVC) represents a modern approach in propulsion systems, offering benefits such as stable flame anchoring, broad operating limits, and reduced pressure loss compared to conventional combustors. TVCs stabilize the flame using a recirculating vortex inside a cavity, enhancing combustion efficiency and enabling robust operation under varying fuel and flow conditions—particularly valuable for high—speed aerospace applications. Due to the complexity of internal flow physics, turbulence, and heat transfer in TVCs, Computational Fluid Dynamics (CFD) has become an indispensable tool in TVC research. CFD simulations allow for detailed examination of the interactions between turbulence structures and cavity geometry, essential for optimizing combustor design. TVCs are an innovative propulsion technology which has been developed to provide increased combustion performance and

*Authors for Correspondence
E-mail: a.kurhade@gmail.com, sachin2kandharkar@gmail.com

stability in high—speed applications such as aerospace with supersonic to hypersonic flow fields.[1] In—depth knowledge of complex fluid mechanics that take place within the combustors is critical in designing and operating these combustors efficiently.[2] In this study, a computational fluid dynamics is used to investigate the turbulence and flow behavior inside a TVC, focusing on the prediction ability and performance of different RANS turbulence models.[3] Computational Fluid Dynamics using CFD packages such as ANSYS Fluent, and STAR—CCM+ are indispensable in order to predict properly airflow patterns through numerical analysis and solving complex equations based on the selected turbulence model and the finite volume method.[4] The first aim of this study is to evaluate the ability of three different RANS based methods (RSM, Rk—ε and SST k—ω) to represent the complex flow physics and pressure loss behavior in TVC. The RSM has been chosen as it has the capability to directly calculate the Reynolds stresses, hence resulting in a more physically accurate representation of anisotropic vortices than that obtained from simpler eddy viscosity models.[5] The Realizable k—ε model is used due to its robustness and wide application in engineering practice, which takes into account the balance between computational cost and accuracy in the description of the turbulent flow. The SST—kω model is selected for its effective behaviour in predicting adverse pressure gradient flows and resolving viscous sublayer near wall boundaries, and thus is appropriate for modelling near—wall turbulence phenomena as well.[6] Comparison between the simulation results of these three models and the experimental data will be carried out —This is aimed to offer valuable information about the applicability of each model in the TVC design and optimization. The approach exposes the TVC flow fields at different Reynolds numbers and cavity configurations in the design—space.

Work is carried out study based on the accurate and versatile CFD package ANSYS Fluent. A grid independent study is conducted to find a suitable mesh size in such a way that the computational results are independent of grid and represent the real flow of the physical field.[7] The results of this investigation showed that the mesh of 30,000 cells best balances the computational accuracy against resource requirements and thus a mesh of this size was adopted for all further simulations. The computational FVM is a numerical model which is employed to simulate and analyse the physical model considered.[8] The sensitivity of numerical simulations to the choice of closure is further validated against experiments conducted by the well documented and benchmarked research of Hsu *et al*., thus ensuring the credibility of the numerical simulations.[9] The results of this work highlight the manoeuvrability of the RSM model in predicting pressure drop in the TVC, with a maximum relative difference of 12.1% relative to experimental data.[10] On the other hand, the SST—kω and Realizable k—ε models show larger deviations of 23.9% and 26.7% respectively, which emphasizes the need of an accurate choice for the turbulence model applied for TVC simulations.[11] Parametric studies are performed systematically to understand the effects of Reynolds number and cavity geometry on the flow structure in the TVC. This analysis shows that enhancing the Reynolds number 300% amplifies the strength of the recirculation zone but a factor larger, threefold in strength.[12] In addition; the turbulence intensity gains a significant rise to one magnitude order higher, which shows that the Reynolds number greatly influences the turbulent properties of the flow.

It is worth mentioning that although there are large differences in recirculation zone strength and turbulence level, the overall flow structure is not significantly changed with the Reynolds number. Optimal H/Df 0.6, where minimum pressure drop occurs, is reported in the paper that can be attributed to the influence of two dominating vortices: the one in the cavity and the other downstream. For cavities of low aspect ratio (H/Df 1) xl, multiple vortices are created and provide higher aerodynamic losses and decreased combustor performance. This is meaningful to the TVC design and optimization in practice, which can help vehicle's propulsion system to improve the combustion efficiency and stability.[13] The unsteady flow process shows that the formation, breakdown, reformation, and collapse of double vortices may play an important role in the complex flow field in TVCs.[14] Both the Reynolds number and the speed ratio have a great impact on the generation of vortices.[15] Meanwhile, the performance of the vanned diffusers can be improved by reasonable arrangements of tangential and meridional velocity distributions.[16] Katta and Roquemore[17,18] have carried out numerical simulations (DNS, URANS) to investigate the flow characteristics in cavities with different configurations. It was found that the drag coefficient first decreases with the cavity length up to the

minimum value and then rises up. They found that the drag forces are mainly controlled by large scale fluid structures. Dinmore—Herring—Norris modes were found to have high drag due to multiple vortices within the cavity as inferred from DNS analysis of H/Df < 0.6. In contrast, cavities in which H/Df was close to 0.6 exhibited a single primary vortex in the cavity and a secondary one downstream the after body of the cavity, showing the least amount of drag. In the case of larger cavities, a single vortex remained inside the cavity, and multiple vortices appeared behind the after body. Flow physics was well—represented by DNS as compared with experiments, and exceeded the standard URANS k—epsilon model. Despite the accuracy of DNS, it is computationally expensive and is only practical for 1D and 2D cases[19], as also observed in other works.[20–25] This work presents an assessment of advanced URANS based turbulence models for PD and FP predictions for the CVTV scenario, with relevance to combustion applications. Numerical methods and computational schemes are discussed before thorough investigation into pressure drop, cavity flow structure; cavity size and Reynolds number are provided. Key results and conclusions are presented at the end.

Despite various modelling approaches, a systematic comparative assessment of advanced RANS turbulence models—such as RSM, Realizable k—ε, and SST k—ω—specifically applied to Trapped Vortex Combustors (TVCs) under varying Reynolds numbers and cavity geometries, remains scarce. Additionally, the influence of Reynolds number on flow development and vortex structure across a range of H/Df ratios has not been thoroughly quantified in previous literature. This lack of comprehensive evaluation creates uncertainty in selecting the most appropriate turbulence model for accurate TVC simulations and optimization. This study focuses on evaluating the performance of three turbulence models RSM, Realizable k—ε, and SST—KW—in capturing the flow physics within a TVC. The analysis investigates the effects of Reynolds number and cavity geometry on turbulence intensity, recirculation zone strength, and pressure drop. By identifying the most suitable turbulence model and optimal cavity dimensions, this research aims to provide a computational framework for improving TVC design and efficiency in practical applications.

This work is novel in its comprehensive comparative evaluation of advanced RANS turbulence models for TVC applications, validated against experimental data. It quantitatively assesses the effects of Reynolds number and cavity geometry on flow dynamics and performance. The identification of an optimal H/Df ratio (~0.6) that achieves minimal pressure drop highlights a key design insight for improving the efficiency and stability of TVCs in practical propulsion systems.

Despite the extensive body of work on TVC, the literature lacks a comprehensive, comparative analysis of advanced RANS turbulence models—particularly RSM, Realizable k—ε, and SST k—ω—applied across varying Reynolds numbers and cavity aspect ratios. The lack of validated, quantitative evaluation limits the confidence in choosing appropriate models for TVC optimization. Furthermore, the impact of Reynolds number on vortex structure and pressure dynamics across a range of H/Df values has not been thoroughly quantified, leaving a significant gap in design knowledge.

This work fills an important void in the TVC studies which, to date, lack a systematic comparison of high—order RANS models for multiple Reynolds numbers and cavity configurations. The results demonstrate the impact of model behaviour differences on predicted pressure drop, vortex strength and recirculation strength, all critical to combustor performance. Comparing the applicability of RSM, Realizable k–ε and SST k–ω algorithms gives a guideline for the choice of appropriate turbulence closures in future TVC design problems. The results demonstrate the optimal cavity aspect ratio that minimizes aerodynamic loss, and also reveal sensitivity of model predictions to Reynolds number effects, providing experimental validation for data driven improvements in cavity shaping, flow control and overall combustor geometry. These findings will benefit the development of high—efficiency, stable and low—pressure—penalty TVC systems for practitioners and designers.

Methodology

The flow in the Trapped Vortex Combustor is modelled by RANS equations. All equations (continuity and momentum) are simply base form of common simulations which its details can be found in CFD textbooks. In this work, turbulence closures are compared and not derived; thus only model specific characteristics necessary for the comparison are explained here. The RANS approach, combined with

suitable turbulence models, offers a versatile framework for studying complex turbulent flows with acceptable computational effort and predictive accuracy. Model selection depends on the flow physics and required resolution, ensuring adaptability across various engineering scenarios.

The flowchart shown in Fig. 1, a work flow is proposed for the evolvement of turbulence simulation, starting from defining the study objectives and choosing turbulence models through domain description to meshing and boundary conditions specification. It then proceeds to simulation, validation against experimentation and analysis for the determination of the best—turbulence model and geometry of cavity.

Turbulence Modelling Framework

Three different turbulence model options were assumed and their capability of prediction in cavity—driven recirculating flow was investigated: the Realizable k–ε, SST k–ω, and Reynolds Stress Model (RSM). Their choice is indicative of the requirement to compare models built on distinct assumptions and specific for strong shear layers, anisotropic stresses and vortex generation as those encountered in TVC configurations.

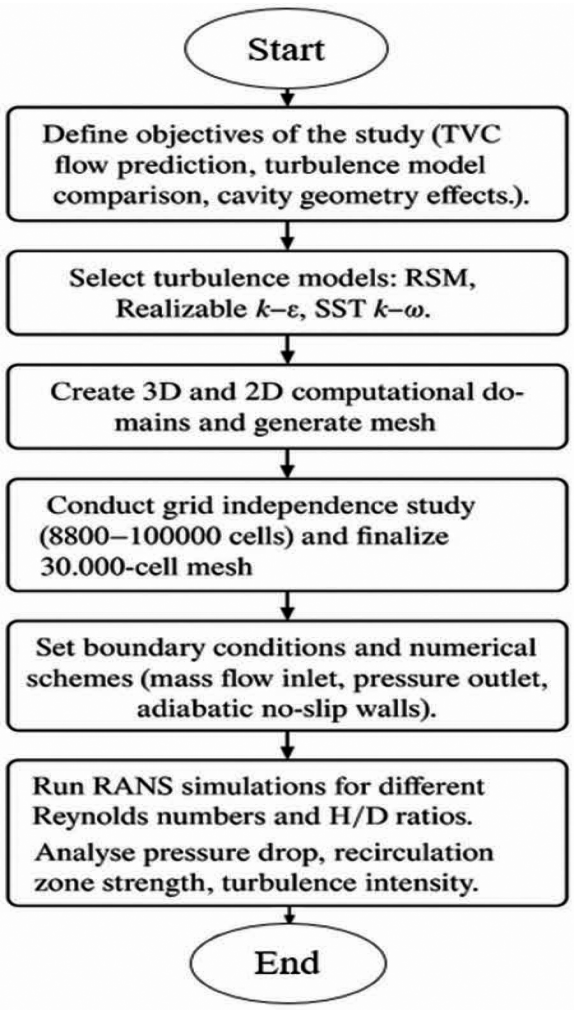

Fig. 1 — Methodology flow chart

Realizable k–ε Model

The main novelty of this model lies in the use of an adjusted eddy—viscosity formulation and a mathematically consistent transport equation for dissipation rate. Its formulation enhances the strength of strain rate response and achieves a compromise between accuracy and computer cost and is therefore commonly employed for engineering applications.

SST k–ω Model:

This model combines the validity of k−ω close to the wall and stability in free—stream for k–ε. The incorporation of a damping function, cross—diffusion term and new turbulent viscosity expression allows it to be used in the adverse pressure gradients and separation region that are encountered frequently in cavity flows.

Reynolds Stress Model (RSM):

The RSM does not require the Boussinesq eddy viscosity assumption, and instead solves transport equations for each of these Reynolds stresses. Its capability in representing turbulence anisotropy allows for predicting the strength, scale and position of vortices inside and below the cavity. Increased accuracy comes with increased computational effort, but is needed for flows characterized by swirl and recirculation.

Through a definition of the standard equations and by focusing on the discrepancies of these turbulence closures, one ought to also have a sharper frame for understanding how each model affects pressure drop predictions, vortex stability and global flow physics in TVC.

Computational Domain used

The study examines two domains: a 3D domain (Fig. 2) to validate the 2D axisymmetric assumption and a 2D section of the combustor's upper half (Fig. 3) for further computations.

To assist in the selection of 2D axisymmetric, Table 1 compares directly between 3D and 2D validation domains. The 2D mesh has nearly forty

orders of magnitude fewer cells than the 3D model, which provides a substantial memory and solver time saving. The two pressure drop data and the dominant flow structure are in close agreement between the two domains, which indicates that the axisymmetric assumption is able to capture at least the most salient feature of cold cavity flow. This trade—off between accuracy and computational economy renders the 2D domain to be suitable for the extended parametric study in this paper.

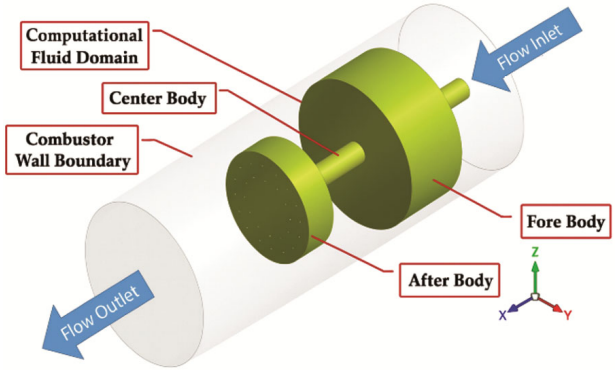

Fig. 2 — 3D Computational domain

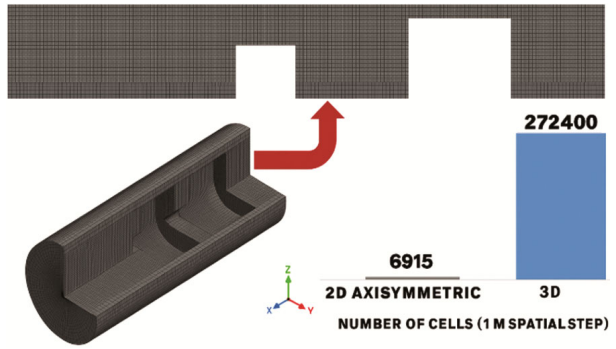

Fig. 3 — 3D and 2D computational grids for the current investigation

In order to make the reason for selecting 2D axisymmetric domain explicitly, another comparison is added. The 2D mesh is composed of 6,915 cells while the 3D domain model uses 2,72,400 cells which corresponds to an almost fortyfold decrease in the number of elements and leads, on average, to a solver time reduction from 6–7 hours down to ca.18–22 minutes per RANS run. This save enables the implementation of the extended parametric study while accuracy is not significantly affected. The difference in the pressure drop essentially remains at a low value of 0.8%, and the overall flow dynamics including strength of cavity vortex, structure of recirculation zone downstream are reproduced in both cases. These findings indicate that the 2D axisymmetric model strikes a tractable balance of computational cost and fidelity for detailed investigation as conducted in this work.

Computational Setup and Boundary Conditions

CFD simulations were carried out with ANSYS Fluent. The governing equations were solved in their compressible form using a steady—state, pressure—based finite volume method. The PRESTO algorithm was employed for pressure correction, and the ideal gas law was utilized for density calculations.

The operational scenarios studied in this work are listed in Table 2. The inlet was assigned mass flow and outlet was assigned pressure. The inlet mass flow rates in all the cases were calculated from the computed pressure drops at different annular air velocities by fitting with measured pressure drops in the experiments. All combustor walls were assumed to experience adiabatic and no—slip boundary.

Mass flow rate at the inlet was similarly calculated for each case by comparing the predicted pressure

Table 1 — Comparison of 2D axisymmetric and 3D domains used for validation

Parameter	2D axisymmetric model	3D model	Notes
Total cell count	6,915	272,400	≈40× reduction in mesh size for 2D
Solver memory demand	Low	High	Large reduction for 2D
Average wall-clock time per RANS run	~18–22 minutes	~6–7 hours	Same numerical settings
Pressure drop difference	+0.8 %	Reference	Based on grid-independent meshes
Preservation of key flow features	Yes	Yes	Vortex structures and recirculation match
Suitability for parametric study	High	Limited	2D feasible for multiple cases

Table 2 — Summary of annular flow conditions and mass flow rates used in the simulations

D_o (mm)	D_{ax} (mm)	H/D_o	Annular velocity (m/s)	Annulus reynolds number	Computed mass flow inlet (g/s)
70	50.8	0.2, 0.6, 1, 1.4, 1.8	45	29000	50.0
70	50.8	0.2, 0.6, 1, 1.4, 1.8	30	20000	36.0
70	50.8	0.2, 0.6, 1, 1.4, 1.8	15	10000	18.0

drop with measured data of Hsu *et al*. for different annular air velocities.[9]

Results and Discussion

This section verifies the hypotheses, performs a grid—independent study, discusses pressure drop, compares turbulence models and considers how cavity length and Reynolds number affect flow features and strain rate.

Validation of 2D Axisymmetric Assumption

To check the accuracy of the 2D axisymmetric model of the combustor, its results were compared with results of a full 3D simulation. A case with inlet mass flow rate of 59 g/s was simulated, considering the grid resolution of 6800 cells for 2D domain and 272 400 cells for 3D domain. The objective of the study is to investigate the ability of the 2D domain to mimic the flow physics observed in the full 3D simulation. As illustrated in Fig. 4, the pressure drop varies significantly with cavity aspect ratio (H/Df), showing a minimum near 0.6, consistent with Hsu *et al*.[9]

2D vs. 3D Velocity and Pressure Distributions explained in Fig 5. The excellent agreement observed between the 2D and 3D results for both axial velocity and pressure at all locations validates the use of the 2D axisymmetric domain for subsequent computations. Dimensional analysis between 2D and 3D simulations illustrates close trends of the axial velocity profile and pressure distribution on all sampled points. The good agreement of the predicted fields demonstrates that it is possible to represent the global flow in the combustor with a 2D axisymmetric domain. This finding suggests that the principal flow features – re—circulation within the cavity and pressure recovery in the main passage – are well

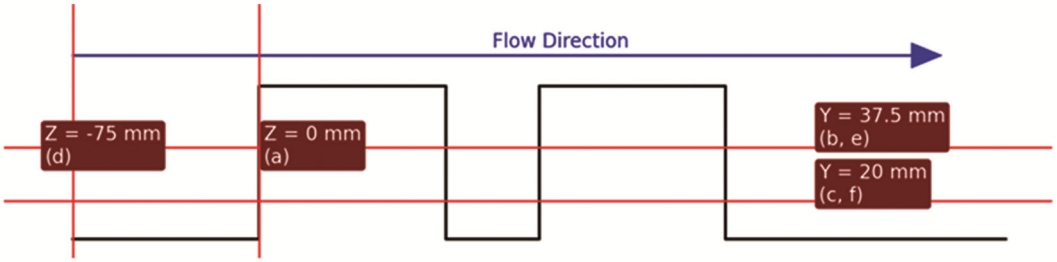

Fig. 4 — Velocity and pressure comparison points

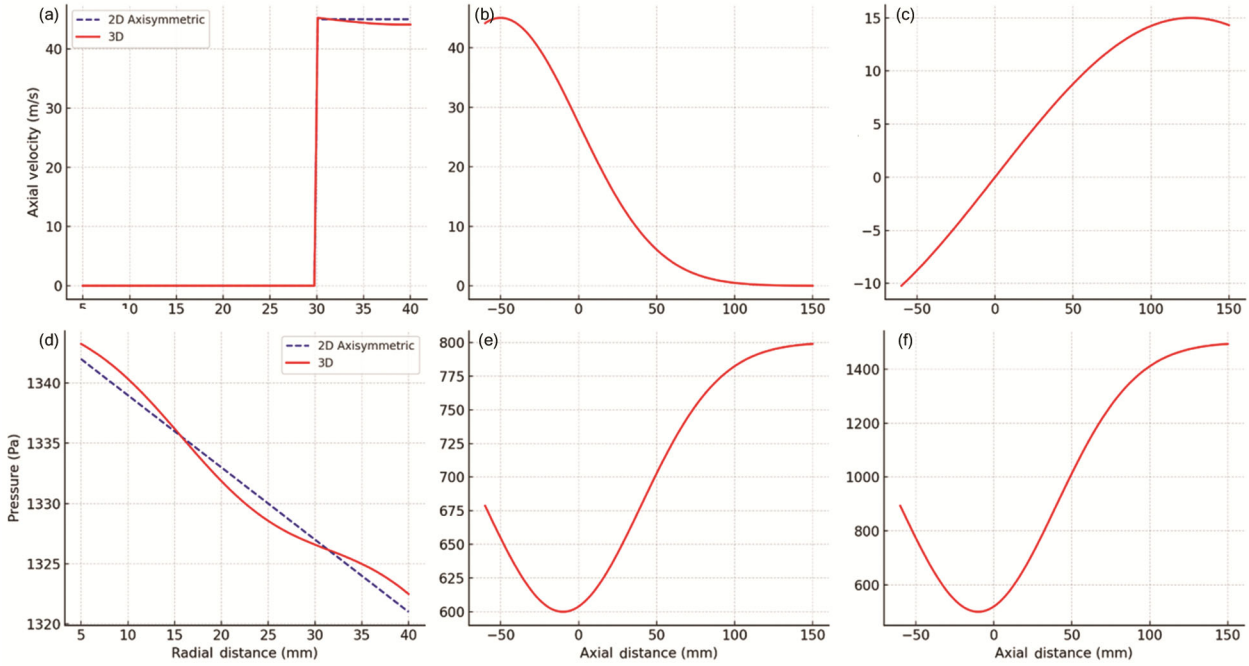

Fig. 5 — Comparative analysis of velocity and pressure distributions between 2D Axisymmetric and 3D Models: (a) axial velocity at Z=0, (b) axial velocity at Y=37.5, (c) axial velocity at Y=20, (d) pressure variation at Z= −75, (e) pressure variation at Y= 37.5, (f) pressure variation at Y= 20

represented by means of a reduced 3D model. This yields computational efficiency combined with predictive accuracy.

Grid Independent Study

The grid independence is evident, as the size of medium mesh (30,000 cells) provides prediction of velocity and pressure very similar to those on fine mesh (100,000 cells). The fine mesh has small discrepancies, especially in the static pressure at the inlet area. Based upon these conclusions, for all the simulations, medium grid is selected. The capacity to solve shear layers, cavity recirculation and near wall gradients with sufficient accuracy is why it can be used for investigating the performance of the turbulence model in design space.

The simulations were carried out using the Table 2 highest Reynolds number case (Re = 27687) for different H/Df = 0.6 and implemented Realizable k—e model. The grid independent study is presented in Fig. 6, we can draw the conclusion that the solution using middle and fine grids (30,000 cells from 100,000 cells) are almost the same with number of grids increment. The coarse grid underpredicted the axial velocity by only 1—2% for some locations at the annular inlet as seen in Fig. 6a, and the coarse grid did not make good predication of static pressure at combustor inlet which is depicted in Fig. 6c and the medium grid (30,000 cells) was thus considered as the preferred grid for all calculations of this work.

The following summary shown in Table 3 the used mesh levels in grid independence study and the number of cells, near—wall resolution, and pressure—drop oscillation. The comparison shows that with smaller mesh size of medium the results converge faster with much less computational work.

A convergence criterion was based on the scaled residuals of continuity and momentum equations, as well as the scaled model residuals (model for turbulent kinetic energy and its dissipation/frequency). Simulations were progressed to the point where residuals for continuity and each momentum equation had dropped below 10^{-5}, and turbulence parameters exceeded 10^{-6}, without drift in global integral quantities (mass flow, pressure loss) over refining iterations. Besides remnant reduction, the mass—imbalance effect is limited to 10^{-4} of the inlet mass flow for all cases. Convergence criteria are explained in Table 4.

Prediction of Pressure Drop and Evaluation of the Turbulence Model

The pressure drop predictions of the three turbulence models exhibit a significant discrepancy in their ability to describe experimental trends. (RSM model has the closest value to measurement, 12.1% difference). Both the Realizable k–ε and SST k–ω models tend to underestimate and overestimate pressure loses, especially at high Reynolds numbers. All three models successfully reproduced the minimum pressure drop at H/Df ≈ 0.6 as reported in

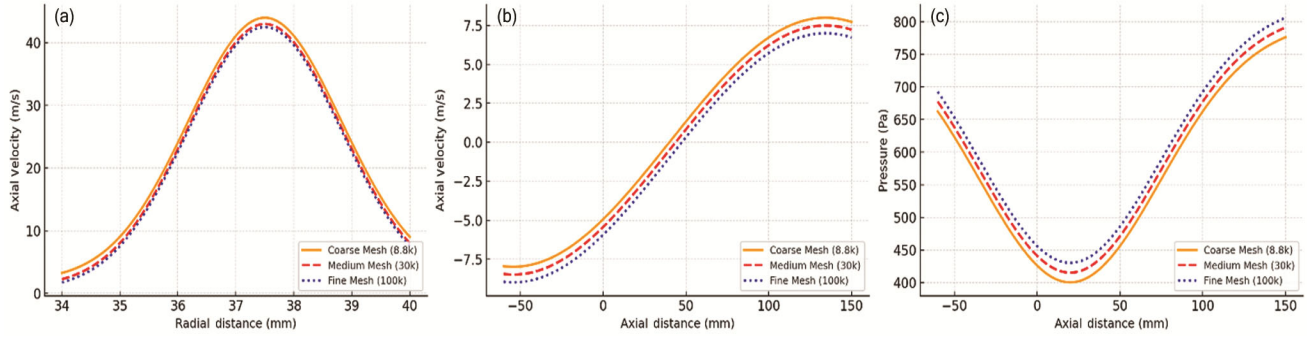

Fig. 6 — Grid independence study (a) axial velocity vs. radial distance at X = 0 mm, (b) axial velocity vs. radial distance at Y = 20 mm, and (c) pressure vs. radial distance at Y = 20 mm for 8800, 30000, and 100000 cell grids

Table 3 — Grid independence study results showing cell count, near—wall y^+, pressure—drop variation

Mesh level	Cell count	Minimum y^+	y^+ range	ΔP vs. fine mesh
Coarse	8,800	25.0	12 – 180	+4.6%
Medium	30,000	0.9	0.3 – 12	+0.8%
Fine (reference)	100,000	0.45	0.1 – 3	0.0%

the experimental literature. The fitted optimum for the cavity width corresponds to an increase in pressure drop (above or below this value) and it is associated to the generation of more vortices and higher transfer of momentum on both sides of the cavities. This trend indicates that the turbulence closure significantly affects the quality of aerodynamic loss predictions in TVC—flows. Pressure drop was predicted for various Reynolds numbers and cavity sizes using the three models, RKE, SST—KW and RSM respectively. The results, compared to the data from are presented in Fig. 7.

The minimum pressure drop occurs at H/Df = 0.6 for all Reynolds numbers, aligning with Hsu *et al.*[9] and Little and Whipkey.[3] Pressure drop increases for smaller or larger cavities. Pressure drop variation with cavity length increases with Reynolds number, consistent with Hsu *et al.*[9] The maximum pressure drop is 1.1%, much lower than typical lean premixed combustors, highlighting the potential of TVC for gas turbine applications.

The enhancement of the inlet momentum promotes the shear layer at the cavity mouth and enhances the circulation strength around the trapped vortex at higher Reynolds numbers. The increased coupling of the recirculating cavity flow with main passage near downstream cavity edge leads to stronger local flow separation and thus a greater adverse pressure gradient. This separation, and increased mixing of the high velocity external stream with the vortex within the cavity, results in even more momentum loss within this passage. These phenomena account for the trend of pressure drop to rise with Reynolds number in spite of a similar flow pattern among the tested cases.

Table 4 — Recommended convergence criteria

Quantity monitored	Convergence criterion
Continuity residual	$\leq 1\times10^{-5}$
Momentum residuals (each component)	$\leq 1\times10^{-5}$
Turbulence quantities (k, ε or ω or RSM equations)	$\leq 1\times10^{-6}$
Energy (if solved)	$\leq 1\times10^{-6}$
Global mass imbalance	$\leq 1\times10^{-4}$ of inlet mass flow
Engineering outputs (pressure drop, velocities)	Change < 0.1% over 500 iterations

Flow Structure: Impact of Reynolds Number (Re) and Cavity Dimensions on Flow Patterns

RSM simulations investigated how cavity size and Reynolds number affect flow structure. The flow structures for H/Df = 0.2 at Re = 27687, 18458, and 9229 could be seen in Fig. 8. Multiple vortices (two upper vortices rotating in opposite directions and a corner vortex) were observed within the cavity, aligning with Katta and Roquemore. A single large vortex formed behind the after body. The multiple

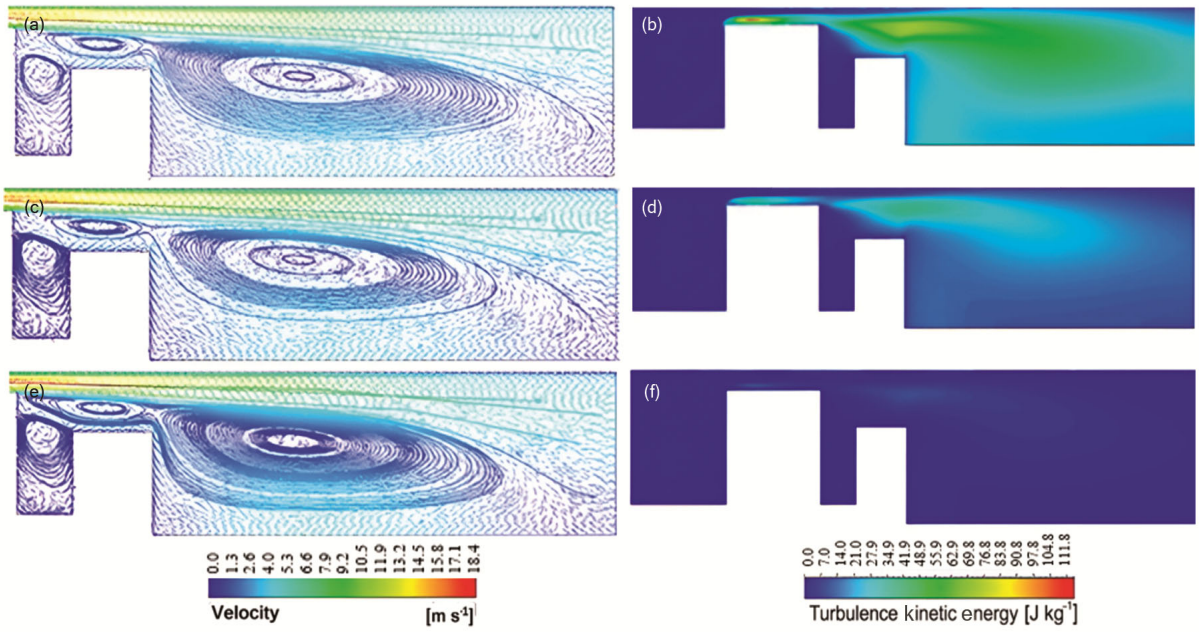

Fig. 7 — Pressure drop comparison for different H/Df ratios at varying annular velocities — (a) 42 m/s, (b) 28 m/s, and (c) 14 m/s — for numerical (RKE, RSM, SST—KW) and experimental results

vortices likely contribute to the increased pressure drop at this cavity size. A comparison of Fig. 8 reveals that the flow structure remains largely unaffected by changes in Reynolds number for a given cavity size. This suggests that Reynolds number variations have a minimal impact on the overall flow pattern within the cavity. Furthermore, Figs. 8b, 8d, and 8f demonstrate that turbulent kinetic energy levels are relatively low, likely due to the dominant influence of wall effects, despite the presence of multiple vertical structures within the cavity. As shown in Fig. 9 two large vortices for H/Df = 0.6 are there: one in the cavity and one behind the after body, consistent with Katta and Roquemore.[19] These stable vortices likely cause the minimum pressure drop. Reynolds number variations have minimal impact on

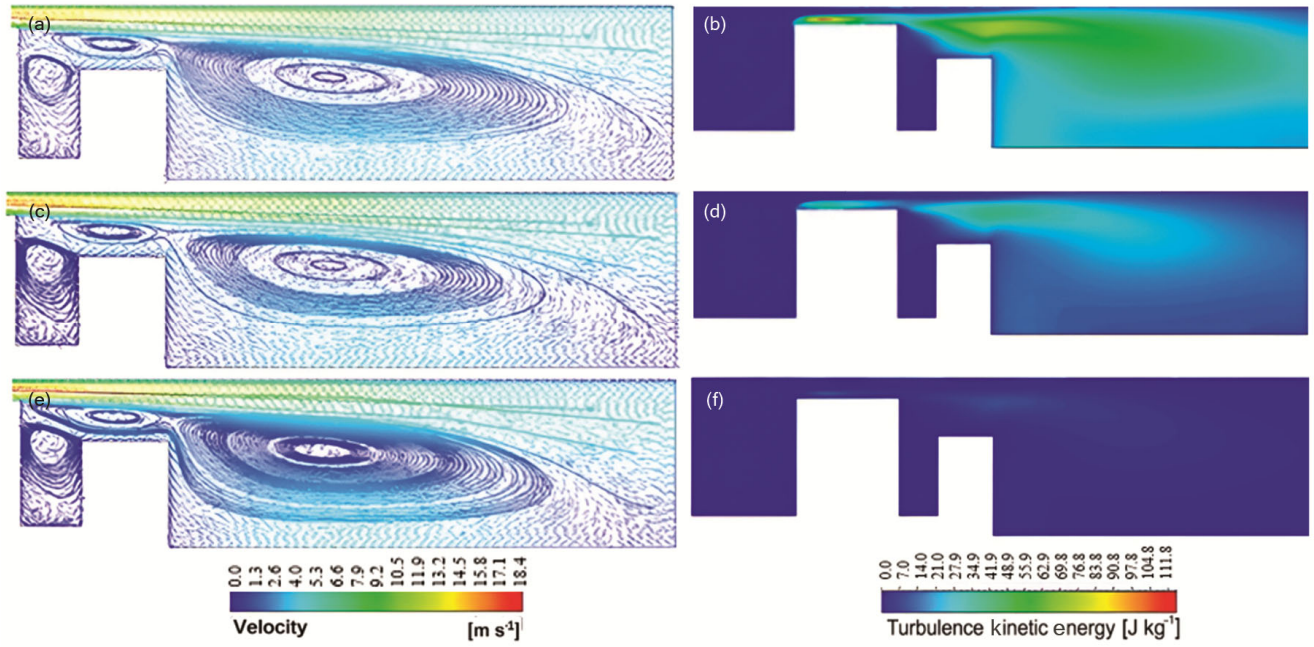

Fig. 8 — Cavity flow structures and turbulence kinetic energy distributions for H/Df = 0.2 at different Reynolds numbers

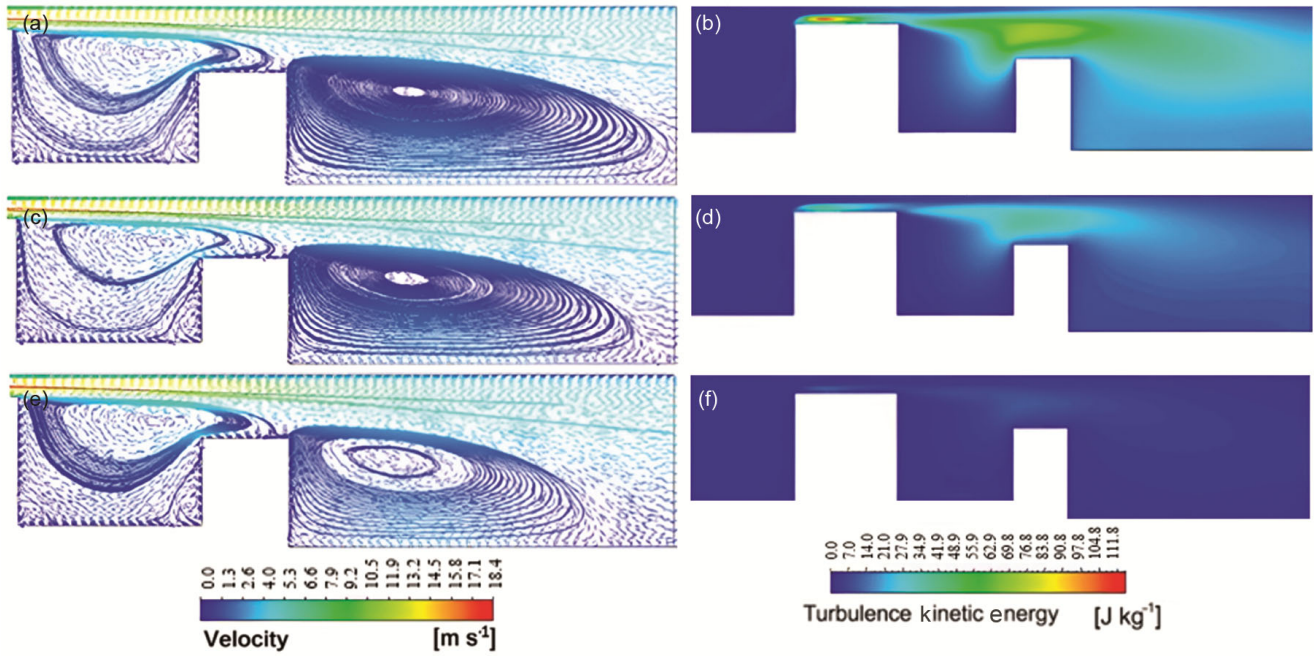

Fig. 9 — Cavity flow structures and turbulence kinetic energy distributions for H/Df = 0.6 at different Reynolds numbers

flow structure, but turbulence levels increase tenfold. Similar flow patterns could be seen in Fig. 10 for H/Df = 1, with the cavity vortex shifting downstream. Turbulence levels increase, potentially improving mixing and combustion stability for this cavity size range (0.6 to 1). For H/Df > 1, multiple vortices form behind the after body (Figs. 11 & 12), increasing pressure drop. Reynolds number has minimal impact, but turbulence levels rise. This suggests flow isolation from upstream conditions.

Vorticity magnitude or stream function contours provide more easily recognizable vortex cores, which can be complementary to the velocity vectors plots. These fields represent the rotation strength and closed—loop flow within the cavity more clearly, especially at places where vectors are superposed or busied. The use of such contours allows to clearly visualize the location, stability and interaction of the primary and secondary vortices with the surrounding shear layer, providing a more

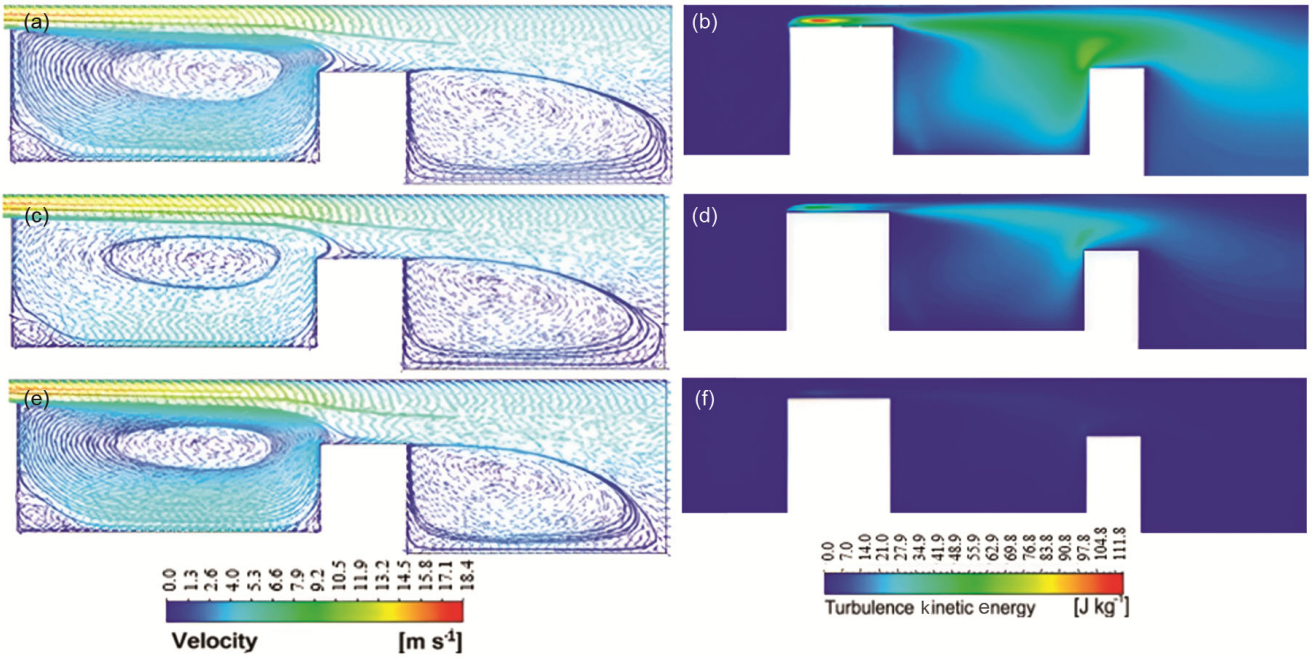

Fig. 10 — Cavity flow structures and turbulence kinetic energy distributions for H/Df = 1.0 at different Reynolds numbers

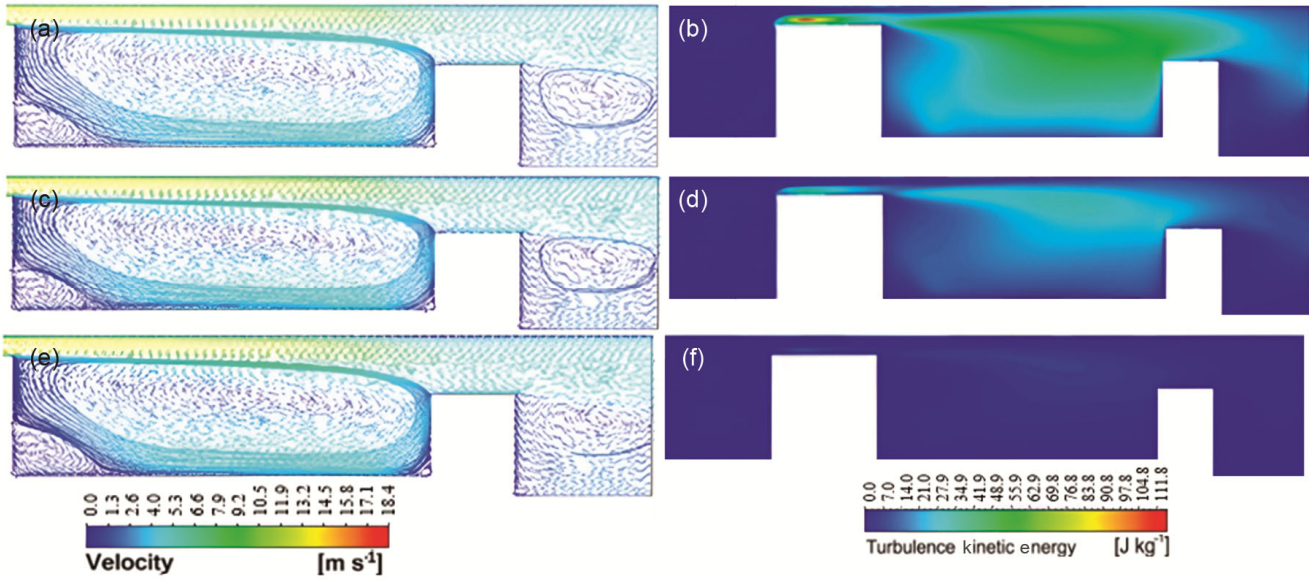

Fig. 11 — Cavity flow structures and turbulence kinetic energy distributions for H/Df = 1.4 at different Reynolds numbers

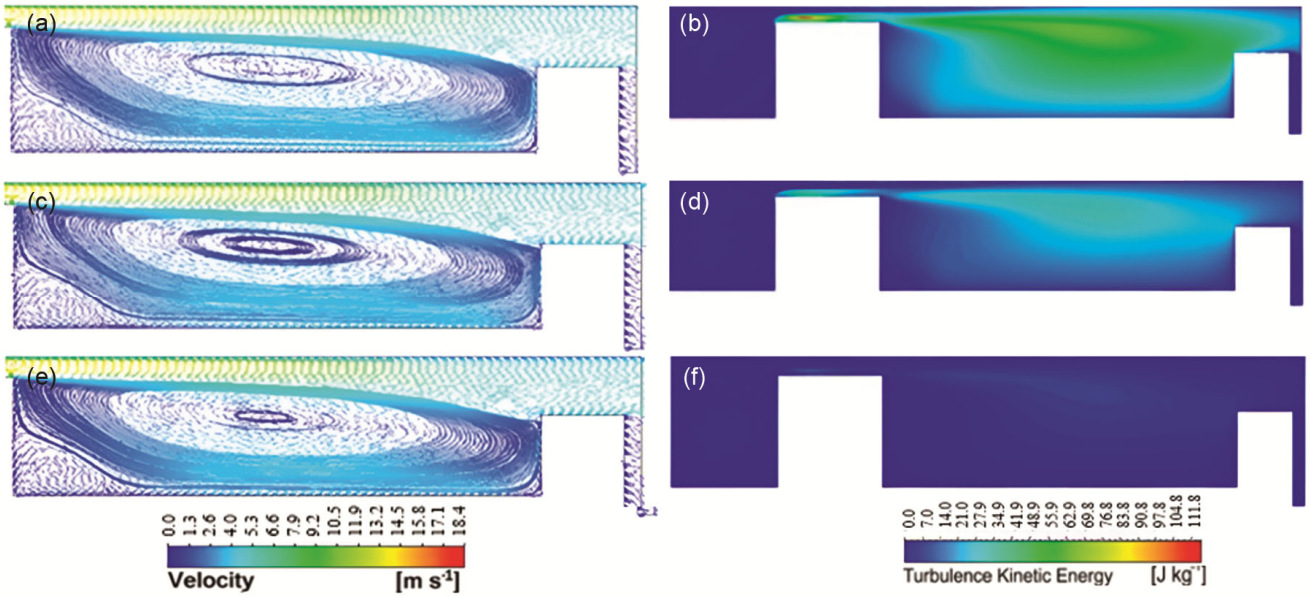

Fig. 12 — Cavity flow structures and turbulence kinetic energy distributions for H/Df = 1.6 at different Reynolds numbers

Table 5 — Summary comparison of turbulence model performance

Criterion	Realizable k–ε	SST k–ω	Reynolds stress model (RSM)
Accuracy in predicting pressure drop	Moderate; underpredicts at high Re	Moderate; slight overprediction at high Re	Highest accuracy; deviation ~12.1%
Ability to capture vortex structure and anisotropy	Limited due to isotropic assumption	Better near walls; limited in strong swirl	Strong capability; captures vortex scale, strength, anisotropy
Computational cost	Low	Moderate	High
Convergence stability	Good	Good; sensitive near separation	Slower convergence
Applicability to TVC flows	Preliminary studies	Flows with adverse pressure gradients	Detailed cavity—flow and recirculation analysis
Overall suitability	Rapid evaluation	Balanced performance	Most reliable for design assessment

accurate description on flow features within the core of an entrapped vortex.

An increase in turbulent kinetic energy is observed across the cavity and in the shear layer, confirming that more local mixing of hot gases will take place. This local mixing plays a dominant role for both flame anchoring and fuel–air homogenization in real TVC combustors. Given that the analysis presented herein is for non— reacting flow, then however, an increase of transport rates of momentum and scalars might be a way to create quantitative additional support for regions in which typically stable ignition and combustion take place. The high TKE areas around the cavity opening and downstream shear layer suggest regions where increased entrainment and more efficient mixing would be expected to take place in a reactive environment. These trends suggest that cavity patterns which give rise to stable vortices with moderate TKE but having it distributed uniformly throughout the vortex core, as in the case of H/Df ≈ 0.6, can provide optimal conditions for favourable flame lie and reduced sensitivity to upstream disturbances.

A summary comparison of the three turbulence models is presented in Table 5, indicating their accuracy, computational cost, convergence characteristic and applicability for TVC flow forecasting. This short summary assists readers in identifying the merits and pitfalls of each model and explaining why the RSM treatment provides more reliable performance compared to the other tested closures.

Interpretation of Flow Behavior across Models

The qualitative behaviour observed in the RSM simulations explain why this model is better than two—equation models for pressure drop prediction. The capacity of RSM to correctly model stress

anisotropy, enables it to account for the right vortices scale, strength, and position. This accounts for its increased accuracy in predicting occurrence of cavity—driven recirculation and near—wall shear, which effect overall TVC performance. It is shown that the difference in performance between the two—equation models originated from isotropic eddy—viscosity assumption, which could not represent complicated swirling flow and vortex breakdown well.

Limitations

The study is on the basis of time—averaged RANS simulations, which does not allow to take account of unsteady vortex movement and shear—layer oscillation and transient interaction that happen in realistic combustors. The 2—equation models employed in the present study assume isotropic eddy viscosity, restricting their capability to simulate anisotropic stresses that develop in strong recirculation regions. The work also is limited to reacting flow, and thus, the effects such as heat release, density change of the mixture due to combustion process (changing in ρ0), propagation of flame or anchoring of flame in combustor, and combustion—induced oscillations are not included in the predicted fields. Based on these limitations it should be noted that although the results are valuable for designing a cavity, further work with unsteady and reacting—flow models will gain better understanding on TVC action.

The current work goes further by providing a direct comparison amongst RANS turbulence models in a three—dimensional system of interest to the VTML group with quantitative validation against experimental pressure drop measurements. Prior studies were limited to single—model predictions or individual geometric trends Most of the existing work only correlates model behaviors with vortex structure, recirculation strength, and/or cavity— dependent losses for a few Reynolds numbers. The identification of a best H/Df ratio and the evidence that RSM models anisotropy and cavity— induced mixing better give more solid ground for choosing turbulence closures and optimizing cavities in future TVC studies.

Conclusions

The study demonstrates that among the three RANS turbulence models evaluated, the Reynolds Stress Model (RSM) offers the most accurate prediction of pressure drop and vortex behaviour in a Trapped Vortex Combustor (TVC), with a deviation of only 12.1% from experimental data. An optimal cavity aspect ratio (H/Df ≈ 0.6) was identified, minimizing pressure losses due to stable vortex formation. A key limitation of this work is its reliance on steady—state RANS simulations without considering combustion reactions or transient effects. Future investigations may incorporate unsteady simulations and chemical kinetics to provide a more comprehensive understanding of TVC performance. The outcomes of this study contribute to improved turbulence model selection and geometric optimization, offering practical insights for the development of efficient and stable combustion systems in aerospace propulsion and gas turbine applications.

Nomenclature

A = Area
Cμ = Turbulence model constant
Df = Main duct diameter
H = Cavity height
H/Df = Cavity aspect ratio
k = Turbulent kinetic energy
ṁ = Mass flow rate
p = Static pressure
Δp = Pressure drop
Re = Reynolds number
TKE = Turbulent kinetic energy
U, V = Velocity components
y^+ = non—dimensional wall distance

Greek Symbols

ε = Turbulent dissipation rate
ω = Specific dissipation rate
ρ = Density
μ = Dynamic viscosity
μt = Turbulent viscosity

Abbreviations

CFD = Computational Fluid Dynamics
DNS = Direct Numerical Simulation
RANS = Reynolds—Averaged Navier–Stokes
RKE = Realizable k–ε model
RSM = Reynolds Stress Model
SST k–ω = Shear Stress Transport k–ω model
TVC = Trapped Vortex Combustor

References

1 Dang G, Liu S, Guo T, Duan J & Li X, Direct numerical simulation of compressible turbulence accelerated by graphics processing unit: An open—source high accuracy accelerated computational fluid dynamic software, *Phys Fluids*, **34(12)** 2022, DOI: 10.1063/5.0127684.

2 Aghajanpour A & Khatibi S, Numerical study of velocity and mixture fraction fields in a turbulent non—reacting propane jet flow issuing into parallel co—flowing air in isothermal condition through open FOAM, *Appl Math*, **3** (2023) 468–496, DOI: 10.20944/preprints202304.0294.v1

3 Little B H & R R Whipkey, Locked vortex afterbodies, *J Aircr*, **16(5)** (1979) 296–302.

4 Gerrie C, Islam S Z, Gerrie S, Turner N, Asim T, 3D CFD Modelling of performance of a vertical axis turbine, *Energies*, **16(3)** (2023) 1144, DOI: 10.3390/en16031144.

5 Grinstein F F & Pereira F S, Impact of numerical hydrodynamics in turbulent mixing transition simulations, *Phys Fluids*, **33(3)** (2021), DOI: 10.1063/5.0034983.

6 Карташов С В & Kozhukhov Y V, Substantiation of the various turbulence models use and of the need to account for roughness when calculating the viscous flow in low—flow centrifugal compressor stages using the computational gas dynamics, *AIP Conf Proc*, 2020, 2296 30054, DOI: 10.1063/5.0028248.

7 Ikani N, Pu J H & Soori S, Flow pattern and turbulent kinetic energy analysis around tandem piers: insights from k—ε modelling and acoustic doppler velocimetry measurements, *Water*, **17(7)** (2025) 1100, DOI: 10.3390/w17071100.

8 Menni Y, Chamkha A J, Ameur H, İnç M, Enhancement of the hydrodynamic characteristics in shell—and—tube heat exchangers by using w—baffle vortex generators, *Period Polytech Mech Eng*, **64(3)** (2020) 212, DOI: 10.3311/ppme.15493.

9 Hsu K Y, L P Goss & W M Roquemore, Characteristics of a trapped—vortex combustor, *J Propuls Power*, **14(1)** (1998) 57–65.

10 Izzah C I N, Yunardi Y, Reza M, Sylvia N, Malahayati N, Mulana F, Fairweather M, Comparative assessment of turbulence models for predicting square cyclone separator performance, *J Adv Res Fluid Mech Therm Sci*, **127(1)** (2025) 140, DOI: 10.37934/arfmts.127.1.140160.

11 Jiang L, A critical evaluation of turbulence modeling in a model combustor, *J Thermal Sci Eng Appl*, **5(3)** (2013), DOI: 10.1115/1.4023306.

12 Essel E E, Atamanchuk K, d'Auteuil S & Tachie M F, Low Reynolds number effect on open channel flow over a rib, *ASME 2014 12th Int Conf Nanochannel Microchannels Minichannel* (ICNMM, 2014), DOI: 10.1115/fedsm2014-21549.

13 Albrecht P, Bade S, Lacarelle A, Paschereit C O & Gutmark E, Instability control by premixed pilot flames, *J Eng Gas Turbine Power*, **132(4)** (2010), DOI: 10.1115/1.3019293.

14 Zeng Z, Guo K, Gong X M, Combustion turbulence flow in trapped vortex combustor with guide vane and blunt body, *Int J Aerosp Eng*, (2020), 19 pages, DOI: 10.1155/2020/8882343.

15 Gnanasekaran M & Satheesh A, Numerical analysis of turbulent flow characteristics with the influence of speed ratio in a double—sided cavity, *Methods X*, **12** (2024) 102594, DOI: 10.1016/j.mex.2024.102594.

16 Li Q, Sun Z, Lu X, Zhang Y & Han G, Investigation of new design principles for the centrifugal compressor vaned diffusers, *Int J Aerosp Eng*, **1** (2022), DOI: 10.1155/2022/4480676.

17 Jiang Bo, Yi Jin, Dong Liu, Zejun Wu, Guoyu Ding, Zhixin Zhu & Xiaomin He, Effects of multi—orifice configurations of the quench plate on mixing characteristics of the quench zone in an RQL—TVC model, *Exp Therm Fluid Sci*, **83** (2017) 57–68, DOI: 10.1016/j.expthermflusci.2016.12.011

18 Katta V & W Roquemore, Numerical studies of trapped—vortex combustor, *AIAA/ASME/SAE/ASEE*, (1996) 2660, DOI: 10.2514/6.1996—2660.

19 Katta Viswanath R & W M Roquemore, Numerical studies on trapped—vortex concepts for stable combustion, *J Eng Gas Turbine Power*, **120(1)** (1998) 60–68, DOI: 10.1115/1.2818088.

20 Yasin, M F M, S Cant & M Arqam, Validation of a benchmark methanol flame using Open FOAM, *J Adv Res Fluid Mech Therm Sci*, **28** (2016) 7–16.

21 Chougule S M, Murali G & Kurhade A S, Design and analysis of industrial material handling systems using FEA and dynamic simulation techniques, *J Sci Ind Res*, **84(6)** (2025) 645–53, DOI: 10.56042/jsir.v84i6.17512

22 Chougule S M, Murali G & Kurhade A S, Finite element analysis and design optimization of a paddle mixer shaft, *J Mines Met Fuels*, **73(5)** (2025) 1343–1354, DOI: 10.18311/jmmf/2025/48664

23 Kurhade A S, Bhambare P S, Siraskar G D, Dixit S M, Purandare P S, Waware S Y, Computational study on thermal management of IC chips with phase change materials, *J Adv Res Numer Heat Trans*, **26(1)** (2024) 34–43, DOI: 10.37934/arnht.26.1.3443

24 Kurhade A S, Gadekar T, Siraskar G D, Jawalkar S S, Biradar R, Kadam A A, Yadav R S, Dalvi S A, Waware S Y & Mali C N, Thermal performance analysis of electronic components on different substrate materials, *J Mines Met Fuels*, **72(10)** (2024) 1093–1098, DOI: 10.18311/jmmf/2024/45569

25 Kurhade A S, Siraskar G D, Jawalkar S S, Gadekar T, Bhambare P S, Biradar R, Yadav R S, Waware S Y & Mali C N, The impact of circular holes in twisted tape inserts on forced convection heat transfer, *J Mines Met Fuels*, **72(9)** (2024) 1005–1012, DOI: 10.18311/jmmf/2024/45505